

DUALITY FOR LEGENDRIAN CONTACT HOMOLOGY

JOSHUA M. SABLOFF

ABSTRACT. The main result of this paper is that, off of a “fundamental class” in degree 1, the linearized Legendrian contact homology obeys a version of Poincaré duality between homology groups in degrees k and $-k$. Not only does the result itself simplify calculations, but its proof also establishes a framework for analyzing cohomology operations on the linearized Legendrian contact homology.

1. INTRODUCTION

1.1. Legendrian Contact Homology. As in smooth knot theory, a fundamental problem in Legendrian knot theory is to find effective invariants and to understand their structure and meaning. Bennequin [1] kick-started the modern study of Legendrian knots by introducing two “classical” invariants: the **Thurston-Bennequin number** (which measures the difference between the framing coming from the contact planes and the Seifert surface framing) and the **rotation number** (which measures the twisting of the tangent to the knot inside the contact planes with respect to a suitable trivialization). These two invariants suffice to classify Legendrian knots in the standard contact structure when the underlying smooth knot type is the unknot [9], a torus knot or the figure eight knot [12], or cable links [7].

The first non-classical invariant of Legendrian knots was **Legendrian contact homology**, which comes from geometric ideas of Eliashberg and Hofer [8, 10] and was rendered combinatorially computable by Chekanov [4] for knots in the standard contact \mathbb{R}^3 . The geometry behind the invariant comes from the Morse-Witten-Floer theory of the action functional on the space of paths that begin and end on a Legendrian knot K . In this setting, Reeb chords correspond to critical points and holomorphic disks in the symplectization $(\mathbb{R}^3 \times \mathbb{R}, d(e^t \alpha))$ take the place of gradient flow lines. In order to ensure $\partial^2 = 0$, the holomorphic disks must be allowed to have multiple negative ends, and the end result is a non-commutative differential graded algebra (DGA) generated by the Reeb chords rather than a graded chain complex. Chekanov’s combinatorial formulation of the DGA arises from the correspondence between Reeb chords and crossings in the xy projection of a Legendrian knot — the Reeb direction in the standard contact \mathbb{R}^3 is the z direction — and between holomorphic disks in the symplectization and immersed disks in the xy projection; see [13] for more details.

It is difficult to extract information from the Legendrian contact homology DGA, but Chekanov defined a linearized version that he used to distinguish

the first examples of Legendrian knots with the same smooth knot type and classical invariants in [4]. The homology of the linearized DGA is usually encoded in a “Poincaré-Chekanov polynomial,” in which the coefficient of t^k denotes the dimension of the linearized homology in degree k . The set of these polynomials taken over all possible linearizations of the DGA is an invariant of Legendrian isotopy class. Though other more powerful — but less computable — methods of mining the DGA have been developed [19], there is still much to be learned about Chekanov’s linearized theory.

Many recent advances in Floer-type theories, and contact homology in particular, have come from importing classical Morse-theoretic ideas. For example, Kálmán’s analysis of nontrivial loops of Legendrian knots was motivated by continuation maps in Morse theory [17]. Another example is the extension of the combinatorial definition of the DGA to knots in circle bundles with contact structures transverse to the fiber, which was achieved by transporting Morse-Bott methods into the contact homology picture [22]; see also Bourgeois’ work on Morse-Bott methods for the non-relative version of contact homology [3].

This paper translates ideas of Betz and Cohen [2] or Fukaya and Oh [16] on gradient flow trees to the construction of a cap product and a “Poincaré duality map” on the linearized DGA. The result is the following theorem:

Theorem 1.1. *The Poincaré-Chekanov polynomial of a linearization of the Legendrian contact homology DGA of a Legendrian knot satisfies:*

$$P(t) = P(t^{-1}) + (t - t^{-1}).$$

This theorem can greatly simplify calculations (see [18], for example), but of greater interest is its proof, which introduces an algebraic and geometric framework for understanding the “algebraic topology” of the linearized DGA. In particular, in the course of proving this theorem, both the “fundamental class” in degree 1 that does not participate in duality and the Poincaré duality maps will be explicitly constructed.

1.2. Morse-Theoretic Motivation. While the proof of Theorem 1.1 will be combinatorial in nature, it is motivated by some geometric ideas from Morse theory. Classically, the Poincaré duality map $D : H^*(M) \rightarrow H_{n-*}(M)$ caps a cohomology class with the fundamental class. Using gradient flow trees as in [2, 16], the cap product and fundamental class can be reinterpreted in the setting of Morse-Witten theory. Recall that the Morse-Witten complex $C_*(M, f)$ of a manifold M with Morse function f is generated by the critical points of f , while the differential comes from counting rigid negative gradient flow lines between critical points; see [24]. The cochain complex $C^*(M, f)$ is generated by the same critical points, but the codifferential counts *upward* gradient flows.

In this language, the fundamental class in is represented by a sum of the maxima. The cap product between a homology class B and a homology class γ is computed by counting certain rigid “Y”-shaped gradient flow trees.

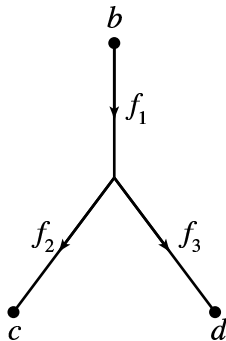


FIGURE 1. A gradient flow tree that gives the cap product $[d] = \gamma \cap B$ between $B = [b]$ and $\gamma = [c]$. Notice that there is one homological input at b , one cohomological input at c , and a homological output at d .

Choose three Morse functions f_1 , f_2 , and f_3 , and choose representatives b for B in $C_*(M, f_1)$ and c for γ in $C^*(M, f_2)$. The “Y”-shaped tree follows the negative gradient flow of f_1 out of b and splits at the vertex into negative gradient flows for f_2 and f_3 . These two flowlines end at c and at a critical point of f_3 that represents $\gamma \cap B$ in $C_*(M, f_3)$, respectively; see Figure 1. By analogy, in the contact homology theory, one might expect the longest Reeb chords to give a fundamental class, and the cap product to come from disks with one positive and two negative ends. These objects will be defined in Sections 4.1 and 4.2, respectively.

In general, gradient flow trees give rise to cohomology operations, with homology inputs and cohomology outputs at the outward-flowing, or “positive,” ends of a negative gradient flow line, and homology outputs and cohomology inputs at the negative ends. Of particular interest in this paper is the inverse of the Poincaré duality isomorphism, which, as Betz and Cohen note, comes from a tree with two positive ends and one vertex, where one of the positive ends is a homology input and the other a cohomology output. The analogy between Legendrian contact homology and Morse theory breaks down here: disks with multiple positive ends do not appear in the contact homology theory. To access disks with two positive ends, it is necessary to expand the algebraic framework of the contact homology DGA. The natural expansion is a relative version of Eliashberg, Givental, and Hofer’s symplectic field theory (SFT) [10]. The definition of a “Legendrian SFT,” however, runs into some subtle issues regarding compactness of the moduli space of curves used to define the differential and has yet to be rigorously defined. Instead, the expansion can be achieved geometrically by embedding a very small copy of a Legendrian knot into the contact circle bundle $(\mathbb{R}^2 \times S^1, d\theta - y dx)$. There are many more Reeb chords in this picture than in the standard contact \mathbb{R}^3 , and some of those chords generate

a cochain complex. The precise nature of this construction will be explored in Section 3.

The remainder of the paper is organized as follows: background notions — including descriptions of Legendrian knot diagrams, the contact homology DGA, rulings, and the linearization procedure — are described in Section 2. Next, Section 3 describes the embedding of the usual linearized DGA into the circle bundle DGA and lays out the structure of the linearized pieces of the latter. The duality maps are defined in Section 4, and Theorem 1.1 is proved modulo some facts about the fundamental class. Finally, Section 5 reviews techniques from [23] that relate augmentations and rulings, and uses the results to prove the existence of a fundamental class.

Acknowledgments. This paper greatly benefited from discussions with John Etnyre, Paul Melvin, Lenhard Ng, and Lisa Traynor. The research behind this paper started out in a rather different direction, and Yasha Eliashberg and Frédéric Bourgeois were instrumental in helping me understand the ideas of symplectic field theory.

2. BACKGROUND NOTIONS

2.1. Legendrian Knots and their Diagrams. This section briefly reviews the basic notions of Legendrian knot theory; for a more comprehensive introduction, see [11, 21].

The **standard contact structure** on \mathbb{R}^3 is the completely non-integrable 2-plane field given by the kernel of $\alpha = dz - y dx$. A **Legendrian knot** is a smooth embedding $K : S^1 \rightarrow \mathbb{R}^3$ that is everywhere tangent to the contact planes. That is, the embedding must satisfy $\alpha(K') = 0$. An ambient isotopy of K through other Legendrian knots is a **Legendrian isotopy**. Legendrian knots are plentiful; for example, any smooth knot can be continuously approximated by a Legendrian knot.

There are two useful projections of Legendrian knots. The first is the **front projection** π_f to the xz plane. In the front projection, the y coordinate of a knot may be recovered from the slope of its projection. As a result, the projection can have no vertical tangencies; it has semi-cubical cusps instead. Further, the crossing information is completely determined: the strand with lesser slope will always pass in front of the strand with greater slope. Any circle in the xz plane that has no vertical tangencies and that is immersed except at finitely many cusps lifts to a Legendrian knot.

A front diagram is in **plat position** if all of the left cusps have the same x coordinate, all of the right cusps have the same x coordinate, and no two crossings have the same x coordinate. The x coordinates of the crossings and cusps are the **singular values** of the front. See, for example, Figure 2(a). Any front diagram may be put into plat position using Legendrian versions of Reidemeister type II moves.

Though the front projection is easier to use, it is more natural to define Legendrian contact homology using the **Lagrangian projection** π_l to the

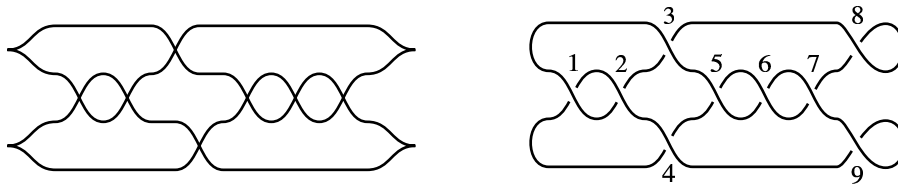


FIGURE 2. The (a) front and (b) Lagrangian diagrams of a Legendrian 5_2 knot. The meaning of the numbers will become clear in Section 2.2.

xy plane. Unlike a front projection, not every immersion into the xy plane is the Lagrangian projection of a Legendrian knot K : a system of inequalities involving the areas of the connected components $\mathbb{R}^2 \setminus \pi_l(K)$ must be satisfied (see [4]). It is simpler (and sufficient) to work with **Lagrangian diagrams** of K , i.e., immersions D of the circle into the xy plane, together with crossing information, for which there is an orientation-preserving diffeomorphism of the plane carrying D to $\pi_l(K)$. See Figure 2(b), for example.

Ng's **resolution** procedure (see [19]) gives a canonical translation from a front projection to a Lagrangian diagram. Combinatorially, there are three steps:

1. Smooth the left cusps;
2. Replace the right cusps with a loop (see the right side of the Lagrangian projection in Figure 2); and
3. Resolve the crossings so that the overcrossing is the one with lesser slope.

A key feature of the resolution procedure is that the heights of the crossings in the Lagrangian diagram strictly increase from left to right, with the jumps in height between crossings as large as desired. In particular, the crossings in a resolved Lagrangian diagram that come from the right cusps have the greatest height among all crossings.

2.2. The Contact Homology DGA in \mathbb{R}^3 . The contact homology DGA was originally defined by Chekanov in [4] for Lagrangian diagrams; see also [13, 19]. This section contains a brief review of the definition.

Let K be an oriented Legendrian knot in the standard contact \mathbb{R}^3 with a generic Lagrangian diagram D . Label the crossings by q_1, \dots, q_n . Let \mathcal{A} be the graded vector space over $\mathbb{Z}/2$ generated by q_1, \dots, q_n , and let \mathcal{A} be the graded free unital tensor algebra TA .¹ The grading is determined by the assignment of a **capping path** to each crossing. A capping path is one of the two immersed paths that starts at the overcrossing of q_i , traces out a portion of D , and ends when D first returns to q_i , necessarily at an undercrossing. Assume, without loss of generality, that the strands of D at

¹It is possible to define the algebra with coefficients in $\mathbb{Z}[T, T^{-1}]$; see [13].

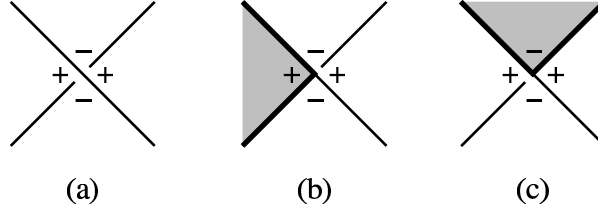


FIGURE 3. (a) A labeling of the quadrants surrounding a crossing; (b) The image of $f \in \Delta$ near the crossing q_i and (c) the crossings q_{j_l} .

each crossing are orthogonal. The **grading** of q_i is defined to be:

$$|q_i| \equiv 2r(\gamma_i) - \frac{1}{2} \pmod{2r(K)}.$$

Extend the grading to all words in \mathcal{A} by letting the grading of a word be the sum of the gradings of its constituent generators.

The next step is to define a differential on \mathcal{A} by counting certain immersions of the 2-disk B^2 with an ordered set of $k+1$ marked points $\{z_0, \dots, z_k\}$ on its boundary. Label the corners of D as in Figure 3(a). The immersions of interest are the following:

Definition 2.1. Given an ordered set of generators $q_i, q_{j_1}, \dots, q_{j_k}$, $\Delta(q_i; q_{j_1}, \dots, q_{j_k})$ is the set of orientation-preserving immersions

$$f : B^2 \rightarrow \mathbb{R}^2$$

up to smooth reparametrization that map ∂B^2 to the image of D subject to the following conditions:

1. The restriction of f to the boundary is an immersion away from the marked points z_i .
2. The map satisfies $f(z_0) = q_i$ and $f(z_l) = q_{j_l}$, with the points $q_i, q_{j_1}, \dots, q_{j_k}$ encountered in counter-clockwise order along the boundary.
3. In a neighborhood of the points $q_i, q_{j_1}, \dots, q_{j_k}$, the image of the disk under f has the form indicated in Figure 3(b,c).

Note the analogy between the positive and negative corners in Figure 3 and positive and negative ends of a gradient flow tree. With this in hand, define the differential as follows:

Definition 2.2.

$$\partial(q_i) = \sum_{f \in \Delta(q_i; q_{j_1}, \dots, q_{j_k})} q_{j_1} \cdots q_{j_k}.$$

Extend ∂ to all of \mathcal{A} via linearity and the Leibniz rule.

The fact that the sum in the definition of ∂ is finite comes from the following lemma, which is essentially an application of Stokes' Theorem:

Lemma 2.3. *Let $h(x)$ be the height of the crossing x . If $\Delta(q_i; q_{j_1}, \dots, q_{j_k})$ is nonempty, then*

$$h(q_i) > \sum_m h(q_{j_m}).$$

The central results in the theory are:

Theorem 2.4 (Chekanov [4]). 1. *The differential ∂ has degree -1 .*
 2. *The differential satisfies $\partial^2 = 0$.*
 3. *The “stable tame isomorphism class” (and hence the homology) of the DGA is invariant under Legendrian isotopy.*

Here, a **stabilization** of \mathcal{A} is a DGA $S(\mathcal{A})$ with two new generators a and b such that $\partial a = b$. Two DGAs \mathcal{A} and \mathcal{A}' are **stable isomorphic** if there exist (possibly multiple) stabilizations of each that are isomorphic; See [4] for a description of the technical condition “tame.”

Example. The knot in Figure 2 has nine crossings. The generators q_1 and q_2 have grading 0; q_3, q_4, q_8 , and q_9 have grading 1; q_5 and q_7 have grading 2; and q_6 has grading -2 . The differential is given by:

$$\begin{aligned} \partial q_1 &= \partial q_2 = \partial q_6 = \partial q_7 = 0 \\ \partial q_3 &= 1 + q_1 q_2 \\ \partial q_4 &= 1 + q_2 q_1 \\ \partial q_5 &= q_3 q_1 + q_1 q_4 \\ \partial q_8 &= 1 + q_1 + q_1 q_6 q_7 \\ \partial q_9 &= 1 + q_1 + q_7 q_6 q_1. \end{aligned} \tag{2.1}$$

2.3. Linearized Contact Homology. Chekanov introduced an important computational technique for Legendrian contact homology called **linearization**. The differential ∂ on \mathcal{A} may be split into a sum of differentials $\partial = \sum_{l=0}^{\infty} \partial_l$, where the image of ∂_0 lies in the ground ring $\mathbb{Z}/2$ and ∂_l maps a generator of A into $A^{\otimes l}$. If $\partial_0 = 0$, then the equation $\partial^2 = 0$ implies $\partial_1^2 = 0$. It follows that (A, ∂_1) is an honest chain complex in this case whose homology $H_*(A, \partial_1)$ may be easily computed.

Rarely does the Legendrian contact homology DGA have the property that $\partial_0 = 0$. Suppose, however, that there exists an algebra map $\varepsilon : \mathcal{A} \rightarrow \mathbb{Z}/2$ that satisfies:

1. $\varepsilon \circ \partial = 0$, and
2. $\varepsilon(q_i) = 0$ if $|q_i| \neq 0$.

Such a map is called an **augmentation**. Augmentations are not uncommon, but they do not always exist; it turns out that their existence is equivalent to the existence of a “ruling” of a front diagram of a Legendrian knot [14, 15, 23]. This equivalence will become important in Section 5, when the fundamental class is fully defined.

Given an augmentation ε , define an automorphism $\Phi^\varepsilon : \mathcal{A} \rightarrow \mathcal{A}$ by:

$$\Phi^\varepsilon(q_i) = q_i + \varepsilon(q_i).$$

Let ∂^ε be the differential induced by Φ^ε :

$$\partial^\varepsilon = \Phi^\varepsilon \partial (\Phi^\varepsilon)^{-1}.$$

It is straightforward to verify that the DGA $(\mathcal{A}, \partial^\varepsilon)$ satisfies $\partial_0^\varepsilon = 0$.

Remark 2.5. Once the augmentation is known, it is possible to read off the linearized differential directly from the Lagrangian diagram. An immersed disk that contributes a q_j to the linearized differential of q_i has a positive corner at q_i , a negative corner at q_j , and possibly other negative corners at augmented crossings. For example, if $\partial q_1 = q_2 q_3$ and only q_2 is augmented, then $\partial_1^\varepsilon q_1 = q_3$. If both q_2 and q_3 are augmented, then $\partial_1^\varepsilon q_1 = q_2 + q_3$. In the latter case, refer to the disk with negative corners at q_2 and q_3 as **totally augmented**.

For each augmentation, there is a **Poincaré-Chekanov Polynomial**:

$$P_\varepsilon(t) = \sum_{n=-\infty}^{\infty} \dim H_l(A, \partial_1^\varepsilon) \cdot t^n.$$

The set $\mathcal{P} = \{P_\varepsilon(t)\}_{\varepsilon \in \mathcal{E}}$ is invariant under Legendrian isotopy, where \mathcal{E} is the set of all possible augmentations of (\mathcal{A}, ∂) . Here is a sketch of a slightly different proof than Chekanov's original in [4]: stabilization does not change the linearized homology, so it suffices to prove that \mathcal{P} is invariant under a (tame) isomorphism. Let $\psi : (\mathcal{A}, \partial) \rightarrow (\mathcal{A}', \partial')$ be an isomorphism, and let \mathcal{E} and \mathcal{E}' denote the sets of augmentations for the domain and range, respectively. There is a bijective correspondence between \mathcal{E} and \mathcal{E}' given by

$$(2.2) \quad \varepsilon' \leftrightarrow \varepsilon = \varepsilon' \psi.$$

It is easy to check that $\Phi^{\varepsilon'} \psi (\Phi^\varepsilon)^{-1}$ conjugates ∂^ε and $(\partial')^{\varepsilon'}$. Further, the correspondence (2.2) can be used to check that the map $\Phi^{\varepsilon'} \psi (\Phi^\varepsilon)^{-1}$ has no constant terms, and hence restricts to a linear isomorphism between $(A, \partial_1^\varepsilon)$ and $(A', (\partial')_1^{\varepsilon'})$. Thus, the correspondence (2.2) induces a bijection between the sets of linearized homologies of (\mathcal{A}, ∂) and $(\mathcal{A}', \partial')$.

Remark 2.6. The set of Poincaré-Chekanov polynomials is not necessarily a one-element set: Melvin and Shrestha [18] found examples of Legendrian knots with arbitrarily large sets.

Example. Referring back to the example in the previous section, it is not hard to check that there is a unique graded augmentation of (\mathcal{A}, ∂) in which both of the degree 0 generators q_1 and q_2 are augmented. The resulting

linearized differential is:

$$\begin{aligned}
 \partial_1^\varepsilon q_1 &= \partial_1^\varepsilon q_2 = \partial_1^\varepsilon q_6 = \partial_1^\varepsilon q_7 = 0 \\
 \partial_1^\varepsilon q_3 &= q_1 + q_2 \\
 \partial_1^\varepsilon q_4 &= q_1 + q_2 \\
 \partial_1^\varepsilon q_5 &= q_3 + q_4 \\
 \partial_1^\varepsilon q_8 &= q_1 \\
 \partial_1^\varepsilon q_9 &= q_1.
 \end{aligned}
 \tag{2.3}$$

An easy computation shows that the linearized homology is generated by $[q_6]$, $[q_7]$, and $[q_8 + q_9]$, so the set of Poincaré-Chekanov polynomials is

$$\{t^{-2} + t + t^2\}.$$

Notice that the Poincaré polynomial in the example is symmetric about degree 0, with the exception of a class in $H_1(A, \partial_1^\varepsilon)$. Theorem 1.1 asserts that this symmetry holds in general.

3. THE EXPANDED ALGEBRA

As suggested in the introduction, the proof of duality for the linearized contact homology DGA requires disks with two positive corners rather than the single positive corner of the disks in Definition 2.1. One method to access these disks is to embed a “small” Legendrian knot in a contact circle bundle. The embedding can be accomplished as follows: given a Legendrian knot K in the standard contact \mathbb{R}^3 , shrink it so that its longest vertical chord has length less than $\delta > 0$. Convert \mathbb{R}^3 into $\mathbb{R}^2 \times S^1$ by modding out by the relation $z \sim z + 2\pi$. Since the standard contact structure is z -invariant, it descends to a contact structure on the circle bundle. Further, the Lagrangian projection π_l to the xy plane still makes sense, and the Reeb direction lies along the fibers.

The embedding of the knot into $\mathbb{R}^2 \times S^1$ introduces many new Reeb chords, and hence many new generators for the contact homology DGA. At each double point of the Lagrangian projection, the old chord that starts on the bottom strand and ends on the top strand is joined by the complementary chord that starts on the top strand and ends on the bottom strand; see Figure 4. There are other new chords that come from composing these chords with multiple copies of the fiber. There are still more chords in the circle bundle picture. At every point on the knot, there is a family of chords that start and end at the same point, traversing the fiber at least once. This seems to indicate that the circle bundle DGA is uncountably generated, but Morse-Bott techniques can be used to localize these chords to isolated points along the knot. The combinatorics of the new chords will be discussed below in Section 3.1. This situation will only use part of the full theory in the circle bundle situation, which was worked out in [22].

A useful property of the complementary chords is that a positive corner for an old chord is a negative corner for the complementary chord. In particular,

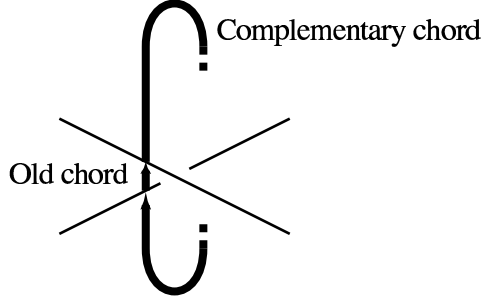


FIGURE 4. Old and (new) complementary chords over a double point of the Lagrangian projection of a small knot in $\mathbb{R}^2 \times S^1$.

disks with multiple positive corners in the original Lagrangian projection appear as genuine contact homology disks in the circle bundle DGA, where one of the “positive” corners is really a negative corner for a complementary chord. Thus, it makes sense to define a cochain complex to the original DGA using the complementary chords, as will be seen in Section 3.2. This section will also describe the structure of the linearized circle bundle algebra.

3.1. Small Knots in $\mathbb{R}^2 \times S^1$.

3.1.1. Generators of the Algebra. The first step in understanding the DGA in the circle bundle setting is to enumerate the generators. As in Section 3 of [22], assume that K has a generic Lagrangian diagram D . On each of the $2n$ edges of the diagram, ordered by an orientation of K , label a point using the ordered set $\{c_1, d_1, \dots, c_n, d_n\}$. Also, choose a direction transverse to D at each c_i ; see Figure 5. The generators of the new algebra are as follows:

- To the i^{th} double point, associate generators $\{q_i^k, p_i^k\}_{k=0,1,\dots}$. The generator q_i^k (respectively, p_i^k) corresponds to the chord that starts on the old bottom (resp. top) strand, winds k times around the fiber, and ends on the old top (resp. bottom) strand. The total length of this chord is on the order of $2\pi k + \delta$ (resp. $2\pi(k+1) - \delta$). The number k is the **level** of the generator.
- To each point c_i , associate generators $\{c_i^k\}_{k=1,2,\dots}$, and to each point d_i , associate generators $\{d_i^k\}_{k=1,2,\dots}$. The generators c_i^k and d_i^k represent the Reeb chords that start and end at the same point and project to the points labeled c_i and d_i , respectively.

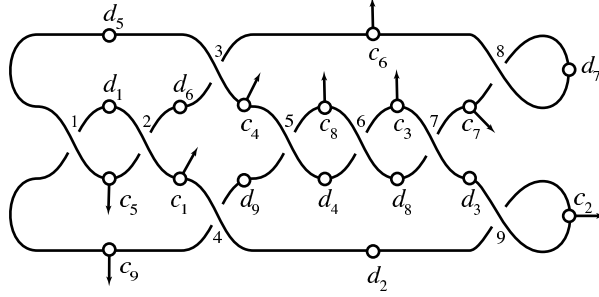


FIGURE 5. The labeling scheme for points on the edges of the Lagrangian projection of K .

It is convenient to organize these generators into formal power series in the variable T :

$$\begin{aligned} \mathbf{q}_i &= \sum_{k=0}^{\infty} q_i^k T^k, & \mathbf{c}_i &= \sum_{k=1}^{\infty} c_i^k T^k, \\ \mathbf{p}_i &= \sum_{k=0}^{\infty} p_i^k T^k, & \mathbf{d}_i &= \sum_{k=1}^{\infty} d_i^k T^k. \end{aligned}$$

For a small knot, the gradings of the new generators are easy to define. Let q_i^0 inherit its grading from the contact homology DGA \mathcal{A} ; the others are graded as follows:

$$(3.1) \quad \begin{aligned} |q_i^k| &= |q_i^0|, & |c_i^k| &= 0, \\ |p_i^k| &= -1 - |q_i^0|, & |d_i^k| &= -1. \end{aligned}$$

Remark 3.1. In the language of [22], these gradings arise from assigning a Maslov index of 0 to the fiber. Since the fiber is homologically nontrivial in the present setting, this assignment corresponds to a choice of trivialization of the contact structure that is invariant under the Reeb flow.

The definition of the contact homology algebra in the circle bundle setting is the same as before: let the **expanded algebra** $\hat{\mathcal{A}}$ be the graded free unital tensor algebra over $\mathbb{Z}/2$ generated by the elements q_i^k , p_i^k , c_i^k , and d_i^k .

3.1.2. The Differential. The extension of the old differential ∂ to $\hat{\mathcal{A}}$ splits into two parts: the “external” differential $\hat{\partial}_{\text{ext}}$, which counts disks similar to those counted by the old differential, and the “internal” differential $\hat{\partial}_{\text{int}}$, which arises from Morse-Bott considerations and counts disks akin to flow-lines along the knot K . As before, it suffices to define the differential on the generators.

First, let us examine the external differential. The disks are almost the same as those used to define the old ∂ , though the conditions at the corners must be changed. The following extension of Definition 2.1 explicitly uses the fact that K is a small knot; see [22] for the general case:

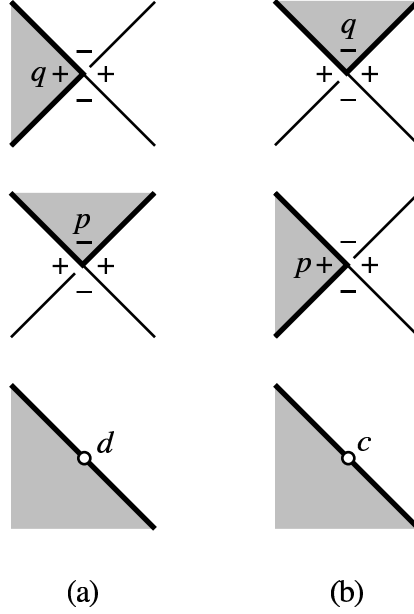


FIGURE 6. The image of $f \in \widehat{\Delta}(\dots)$ near (a) the positive (x) corners and (b) the negative (y_i) corners, depending on whether the label is q , p , c , or d .

Definition 3.2. Given an ordered set of labels $\{x, y_1, \dots, y_l\}$, where $x \in \{q_i, p_i, d_i\}$ and $y_j \in \{q_i, p_i, c_i\}$, $\widehat{\Delta}(x; y_1, \dots, y_l)$ is the set of orientation-preserving immersions that satisfy analogous conditions to those in Definition 2.1 except for the last one, which is replaced by:

- (3) In a neighborhood of the points x, y_1, \dots, y_l , the image of the disk under f has the form indicated in Figure 6.

Care must be taken to ensure that the lift of $f(\partial D^2)$ to K , together with the Reeb chords, actually bound a disk. To this end, introduce a quantity ν_z that is 1 if and only if z is a p label, and define:²

$$(3.2) \quad \nu(x; y_1, \dots, y_k) = -\nu_x + \sum \nu_{y_i}.$$

Definition 3.3. The **external differential** $\widehat{\partial}_{\text{ext}}$ of a generator $x^m \in \widehat{\mathcal{A}}$ is the coefficient of T^m in the expression

$$\sum_{f \in \widehat{\Delta}(x; y_1, \dots, y_k)} \tilde{y}_1 \cdots \tilde{y}_k T^{\nu(x; y_1, \dots, y_k)},$$

²See the discussion after Definition 3.6 in [22] for the genesis of ν .

where

$$\tilde{\mathbf{y}} = \begin{cases} (1 + \mathbf{c}_j)^{-1} & y = c_j \text{ and the transversal at } c_j \text{ points out of the disk;} \\ 1 + \mathbf{c}_j & y = c_j \text{ and the transversal at } c_j \text{ points into the disk;} \\ \mathbf{y} & \text{otherwise.} \end{cases}$$

Extend $\widehat{\partial}_{\text{ext}}$ to all of $\widehat{\mathcal{A}}$ via linearity and the Leibniz rule.

Example. To illustrate how to compute the external differential, return to the example from Sections 2.2 and 3.1 and concentrate on the sixth crossing. Place c and d labels on the diagram as in Figure 5. The differentials for q_6^m and p_6^m can be computed using the following power series:

$$\begin{aligned} \widehat{\partial}_{\text{ext}} \mathbf{q}_6 &= (1 + \mathbf{c}_8)^{-1} \mathbf{p}_5 T + \mathbf{p}_7 (1 + \mathbf{c}_3)^{-1} T; \\ \widehat{\partial}_{\text{ext}} \mathbf{p}_6 &= (1 + \mathbf{c}_3) \mathbf{q}_7 (1 + \mathbf{c}_7)^{-1} \mathbf{p}_8 (1 + \mathbf{c}_6)^{-1} (1 + \mathbf{c}_5) \mathbf{q}_1 (1 + \mathbf{c}_9)^{-1} (1 + \mathbf{c}_8) \\ &\quad + (1 + \mathbf{c}_4)^{-1} \mathbf{q}_1 (1 + \mathbf{c}_1) \mathbf{p}_9 \mathbf{q}_7. \end{aligned}$$

In particular, note that:

$$(3.3) \quad \begin{aligned} \widehat{\partial}_{\text{ext}} q_6^1 &= p_5^0 + p_7^0 \quad \text{and} \\ \widehat{\partial}_{\text{ext}} q_6^2 &= c_8^1 p_5^0 + p_5^1 + p_7^0 c_3^1 + p_7^1. \end{aligned}$$

The disks that contribute to the external differential satisfy the following generalization of Lemma 2.3:

Lemma 3.4. *Let $l(x)$ denote the length of the chord x . If $\widehat{\Delta}(x; y_1, \dots, y_k)$ is nonempty, then:*

$$l(x^m) > \sum_{j=1}^k l(y_j^0) + m + \nu.$$

The **internal differential** is defined as follows: at a crossing, designate q^k by a^k and p^k by b^k if the crossing is configured as in Figure 7(a), and the opposite in the configuration in Figure 7(b). Let d and \bar{d} be the adjacent points as in the figure, and suppose that the configuration around a c point is as in Figure 8. Then define the internal differential as follows, where the internal differential of x^m is understood to be the coefficient of T^m on the right hand side:

$$(3.4) \quad \begin{aligned} \widehat{\partial}_{\text{int}} \mathbf{a} &= \mathbf{a} \bar{\mathbf{d}} + \mathbf{d} \mathbf{a}, \\ \widehat{\partial}_{\text{int}} \mathbf{b} &= \mathbf{b} \mathbf{d} + \bar{\mathbf{d}} \mathbf{b} + \mathbf{b} \mathbf{a} \mathbf{b} T, \\ \widehat{\partial}_{\text{int}} \mathbf{c} &= (1 + \mathbf{c})(\bar{\mathbf{d}}_1 + \mathbf{b}_1 \mathbf{a}_1 T) + (\bar{\mathbf{d}}_2 + \mathbf{b}_2 \mathbf{a}_2 T)(1 + \mathbf{c}), \text{ and} \\ \widehat{\partial}_{\text{int}} \mathbf{d} &= \mathbf{d} \mathbf{d}. \end{aligned}$$

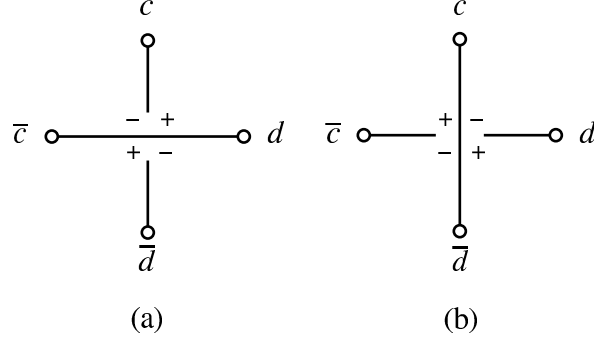


FIGURE 7. In configuration (a), q^k corresponds to a^k and p^k to b^k in the definition of the internal differential. The opposite holds in configuration (b).

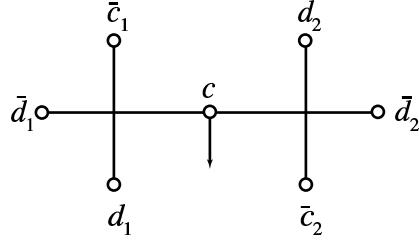


FIGURE 8. The configuration for the internal differential of c^k in equation (3.4).

Note that if the relative positions of the \bar{c}_1 and d_1 on the leftmost vertical strand in Figure 8 are reversed, then $\mathbf{b}_1\mathbf{a}_1$ becomes $\mathbf{a}_1\mathbf{b}_1$, and similarly on the right.

Example. Continuing the previous example, comparing Figures 5 and 7 shows that q_6 is an a generator and p_6 is a b generator. Thus, the equations (3.4) imply that:

$$(3.5) \quad \begin{aligned} \hat{\partial}_{\text{int}}\mathbf{q}_6 &= \mathbf{q}_6\mathbf{d}_4 + \mathbf{d}_8\mathbf{q}_6; \text{ and} \\ \hat{\partial}_{\text{int}}\mathbf{p}_6 &= \mathbf{p}_6\mathbf{d}_8 + \mathbf{d}_4\mathbf{p}_6 + \mathbf{p}_6\mathbf{q}_6\mathbf{p}_6T. \end{aligned}$$

Putting the internal and external differential together yields the full differential for a Legendrian knot in a circle bundle:

Definition 3.5. $\hat{\partial} = \hat{\partial}_{\text{int}} + \hat{\partial}_{\text{ext}}$.

Theorem 3.6 ([22]).

1. The full differential has degree -1 ;
2. The differential satisfies $\hat{\partial}^2 = 0$.
3. The “stable tame isomorphism class” (and hence the homology) of the DGA is invariant under Legendrian isotopy.

3.2. Structure of the Linearized Expanded Algebra. For a small knot in $\mathbb{R}^2 \times S^1$, the set of Reeb chords that run around the fiber between k and $k+1$ times split into two families: short chords with length close to $2\pi k$ and longer chords with length close to $2\pi(k+1)$. Algebraically, this split is realized by the following decomposition of the linear pieces of $\hat{\mathcal{A}}$: let Q^m be the vector space generated by the level m generators $\{q_i^m, c_i^m, d_i^m\}$, where it is understood that $Q^0 = A$. Let $Q = \bigoplus Q^m$. Similarly, define P^m to be the vector space generated by $\{p_i^m\}$, and let $P = \bigoplus P^m$. The goal of this section is to understand the relationships between the Q^m and P^m once $\hat{\mathcal{A}}$ has been linearized.

The first step will be to extend an augmentation for \mathcal{A} to all of $\hat{\mathcal{A}}$. Given an augmentation ε of \mathcal{A} , there is a trivial extension to a map $\hat{\varepsilon}$ on $\hat{\mathcal{A}}$: simply set $\hat{\varepsilon}$ to be zero on all generators not in Q^0 . This map turns out to be an augmentation for the expanded algebra:

Proposition 3.7. $\hat{\varepsilon} \circ \hat{\partial} = 0$.

Proof. The first step is to show that, when restricted to Q^0 , $\hat{\partial} = \partial$. Let $q \in Q^0$. Since the Reeb chords that generate Q^0 are shorter than any other chords, Lemma 3.4 implies $\hat{\partial}(q)$ contains only other generators from Q^0 . Said another way, any disk that contributes to $\hat{\partial}(q)$ must have a positive corner at q and all other corners must be negative. This is equivalent to the definition of the disks that contribute to $\partial(q)$. Thus, on Q^0 , $\hat{\partial} = \partial$ and the proposition follows by the definition of $\hat{\varepsilon}$.

For the remainder of the proof, the strategy is to show that every other term in $\hat{\partial}$ contains at least one generator not in Q^0 . By inspection, every term in the internal differential contains such a generator, so

$$\hat{\varepsilon} \circ \hat{\partial}_{\text{int}} = 0.$$

On P , every term in the external differential must contain at least one generator from P . Otherwise, there would be a disk in the original Lagrangian diagram of K , all of whose corners are negative; this is impossible by Lemma 2.3. For a term in the external differential of a generator q in Q^m , $m \geq 1$, two things can happen: either the term contains a generator from P , or else $\nu = 0$ and the term contains at least one element in Q^k , $k \geq 1$. In either case, the term contains a generator that does not lie in Q^0 . \square

The linearized differential $\hat{\partial}_1^{\hat{\varepsilon}}$ can be split into three pieces by restricting domains and ranges. For convenience, the superscript $\hat{\varepsilon}$ will be dropped from the notation henceforth, i.e., all differentials will be assumed to be augmented. The linearized differential splits into three pieces:

1. $\hat{\partial}_Q : Q \rightarrow Q$ comes from restricting the domain and range of $\hat{\partial}_1$ to Q ;
 2. $\hat{\partial}_P : P \rightarrow P$ comes from restricting the domain and range of $\hat{\partial}_1$ to P ;
- and

3. $\eta : Q \rightarrow P$ comes from restricting the domain of $\widehat{\partial}_1$ to Q and its range to P .

Notice that there is no piece of the linearized differential with domain P and range Q ; as was proved in Proposition 3.7, on P^m , every term in the external differential must contain at least one generator from P^k , $k \leq m$. Thus, it is possible to represent $\widehat{\partial}_1 : Q \oplus P \rightarrow Q \oplus P$ by the following matrix:

$$\begin{bmatrix} \widehat{\partial}_Q & 0 \\ \eta & \widehat{\partial}_P \end{bmatrix}.$$

The domains and ranges of $\widehat{\partial}_Q$, $\widehat{\partial}_P$, and η can be further refined, giving two families of linear chain complexes:

Proposition 3.8. 1. $(Q^m, \widehat{\partial}_Q)$ and $(P^m, \widehat{\partial}_P)$ are chain complexes, and
 2. $\eta : (Q^m, \widehat{\partial}_Q) \rightarrow (P^{m-1}, \widehat{\partial}_P)$ is a chain map for $m \geq 1$.

Proof. Implicit in the statement of the proposition is the claim that both $\widehat{\partial}_Q$ and $\widehat{\partial}_P$ preserve levels, and η reduces the level by 1. To prove the claim, consider a term $\mathbf{y}_1 \cdots \mathbf{y}_k T^\nu$ in the power series formula for $\widehat{\partial}x^m$. A monomial in the expansion of this term will contribute to the linearized differential if and only if all but at most one of its constituent generators is augmented. By the definition of $\widehat{\varepsilon}$, then, at most one of the constituent generators of the monomial will have nonzero level, and this level will be $m - \nu$. Thus, to prove the claim, it suffices to show that $\nu = 0$ for any term in the power series formulae for $\widehat{\partial}_Q(x^m)$ or $\widehat{\partial}_P(x^m)$, and that $\nu = 1$ for $\eta(x^m)$.

To prove the necessary facts about ν for terms coming from the external differential, equation (3.2) needs to be examined. In all cases, the augmented generators among the y_i live in Q^0 , and hence do not contribute to ν . Thus, it suffices to compare the values of ν on x and on its image y under $\widehat{\partial}_Q$, $\widehat{\partial}_P$, and η . For $\widehat{\partial}_Q$ and $\widehat{\partial}_P$, compute as follows:

$$\nu = \nu_y - \nu_x = 0 - 0 = 0.$$

For η , this becomes:

$$\nu = \nu_y - \nu_x = 1 - 0 = 1.$$

This proves the claim for terms coming from the external differential.

Referring to (3.4) for the internal differential, it is easy to see that the only way the internal differential can contribute a linearized term in the a (respectively, b) cases is if a^0 (resp. b^0) itself is augmented. In that case, a^m (resp. b^m) lies in Q^m , and the first two terms in the first two equations in (3.4) contribute to $\widehat{\partial}_Q$ with $\nu = 0$. The last term in the internal differential of b^m contributes to η with $\nu = 1$. The claim follows in these cases, and similar considerations hold for c^m . In fact, it can be seen that

$$(3.6) \quad \widehat{\partial}_Q(c^m) = d^m + \bar{d}^m,$$

where d and \bar{d} are adjacent to c along the knot. Note that the **ab** terms contribute to $\eta(c^m)$.

Lastly, since d^m can never be augmented, the linearized internal differential of d^m must be zero. In passing, this observation, combined with the fact that d^m has trivial external differential, proves:

$$(3.7) \quad \widehat{\partial}_Q(d^m) = 0.$$

This proves the claim for terms coming from the internal differential.

With the claim in hand, the proposition follows easily from the following calculation:

$$0 = \widehat{\partial}_1^2 = \begin{bmatrix} \widehat{\partial}_Q & 0 \\ \eta & \widehat{\partial}_P \end{bmatrix}^2 = \begin{bmatrix} \widehat{\partial}_Q^2 & 0 \\ \eta\widehat{\partial}_Q + \widehat{\partial}_P\eta & \widehat{\partial}_P^2 \end{bmatrix}.$$

□

Example. As noted in the example in Section 2.2, the only generators augmented in the case of the knot in Figure 2 are q_1^0 and q_2^0 . Thus, for q_6 and p_6 , the internal differential contributes nothing to the linearized differential. Further, it is straightforward to read off that $\widehat{\partial}_Q(q_6^m) = 0$ and $\widehat{\partial}_P(p_6^m) = 0$ for all $m \geq 0$. The η map at this crossing, however, is nontrivial:

$$(3.8) \quad \eta(q_6^m) = p_5^{m-1} + p_7^{m-1}.$$

There is a “vertical” relationship between the complexes $(Q^m, \widehat{\partial}_Q)$ and $(Q^{m+1}, \widehat{\partial}_Q)$. This relationship can be encoded by a **translation map** $\tau : Q^m \rightarrow Q^{m+1}$ that sends x^m to x^{m+1} ; a similar map exists for P . The translation map interacts nicely with the linearized differential:

Lemma 3.9. *The translation map τ is a chain isomorphism on $(P^m, \widehat{\partial}_P)$, $m \geq 0$, and on $(Q^m, \widehat{\partial}_Q)$, $m \geq 1$. Further, τ commutes with η .*

Proof. As noted in the proof of Proposition 3.8, the only monomials in the expansion of the power series that can contribute to the linearized differential $\widehat{\partial}_Q(x^m)$ or $\widehat{\partial}_P(x^m)$ are those of the form

$$(3.9) \quad q_{j_1}^0 \cdots q_{j_l}^0 y^m q_{j_{l+1}}^0 \cdots q_{i_k}^0,$$

where each $q_{j_i}^0$ is augmented; a similar fact holds for η with y^m replaced by y^{m-1} . For all levels in P and for levels greater than zero in Q , the translation map τ is obviously bijective. Since the power series formulae for $\widehat{\partial}(x^m)$ and $\widehat{\partial}(x^{m+1})$ are identical and $\nu \leq 1$, there is a bijective correspondence between terms in $\widehat{\partial}(x^m)$ as in (3.9) with y^m and terms in $\widehat{\partial}(x^{m+1})$ with y^{m+1} . □

More interesting phenomena occur when comparing $(Q^0, \widehat{\partial}_Q) = (A, \partial)$ to $(Q^1, \widehat{\partial}_Q)$. The issue here is that the terms coming from equation (3.9) contribute identically (up to a translation) to $\widehat{\partial}_Q(q^0)$ and $\widehat{\partial}_Q(q^1)$, but $\widehat{\partial}_Q(q^1)$ can have extra terms when y is a c or d generator. This is not an issue when

the degree of q is not 0 or 1; the proof of the lemma above therefore shows that

$$(3.10) \quad \dim H_k(Q^1, \widehat{\partial}_Q) = \dim H_k(A, \partial)$$

for $k > 1$ and $k < -2$.

In degree -1 , it turns out that

$$(3.11) \quad \dim H_{-1}(Q^1, \widehat{\partial}_Q) = \dim H_{-1}(A, \partial) + 1.$$

In the following proof of (3.11), let Q_k^m be the degree k part of Q^m . To begin with, the kernel of $\widehat{\partial}_Q$ on Q_{-1}^1 is the sum of the translated kernel of $\widehat{\partial}_Q$ on Q_{-1}^0 and the subspace of Q^1 generated by all d^1 generators. The image of $\widehat{\partial}_Q$ on Q_0^1 differs from that on Q_0^0 in two respects: first, the c^1 terms have a linearized differential given by equation (3.6). Second, if q^0 is augmented, the corresponding q^1 terms have a contribution of $d^1 + \bar{d}^1$ to their linearized differential given by the internal differential. To incorporate this information, let γ_i be the sum of the c^1 generators that lie on a capping path of q_i . Change basis in Q_0^1 so that if q_i^0 is augmented, then q_i^1 is replaced by $q_i^1 + \gamma_i$. In this basis, it is clear that the image of $\widehat{\partial}_Q$ is the sum of the translation of the image of $\widehat{\partial}_Q$ on Q_0^0 and the subspace of Q_{-1}^1 generated by $\{d_i^1 + d_{i+1}^1\}_{i=1, \dots, n-1}$. Thus, the degree -1 homology of Q^1 is the same as that for Q^0 with the addition of the class $[d_1^1] = [d_2^1] = \dots = [d_n^1]$. Equation (3.11) follows.

Finally, consider degree -2 . The kernels of $\widehat{\partial}_Q$ on Q_{-2}^0 and Q_{-2}^1 agree up to a translation, and equation (3.7) shows that the image of $\widehat{\partial}_Q$ on Q^0 agrees with the image of $\widehat{\partial}_Q$ on Q^1 up to a translation. Thus,

$$(3.12) \quad \dim H_{-2}(Q^1, \widehat{\partial}_Q) = \dim H_{-2}(A, \partial).$$

There is also a “horizontal” relationship between the chain complexes $(Q^0, \widehat{\partial}_Q)$ and $(P^0, \widehat{\partial}_P)$. Define a degree 1 pairing³ on $P^0 \otimes Q^0$ by:

$$\langle p_i, q_j \rangle = \delta_{ij}.$$

This pairing allows us to view $(Q^0, \widehat{\partial}_Q)$ and $(P^0, \widehat{\partial}_P)$ as dual complexes since a disk that contributes q_j to $\widehat{\partial}_Q(q_i)$ also contributes p_i to $\widehat{\partial}_P(p_j)$. Since the internal differential is zero at level zero, the following lemma is immediate:

Lemma 3.10. *With respect to the pairing \langle, \rangle , $(P^0, \widehat{\partial}_P)$ is the dual chain complex of $(Q^0, \widehat{\partial}_Q)$. In particular, by (3.1),*

$$\dim H_k(Q^0, \widehat{\partial}_Q) = \dim H_{-k-1}(P^0, \widehat{\partial}_P).$$

Example. Combining the lemma with equation (2.3) shows that p_7^m represents a non-trivial homology class and that p_5^m is a boundary in $(P^m, \widehat{\partial}_P)$.

³This assumes that the base ring lies in degree 0.

Thus, since η is a chain map, (3.8) becomes:

$$(3.13) \quad \eta_*[q_6^m] = [p_7^{m-1}].$$

4. THE CAP PRODUCT AND DUALITY

The expanded algebra defined in the previous section provides the structure with which to prove duality. The important ingredients in actually proving Theorem 1.1 are:

1. The fundamental class, derived from chords of maximum height in Section 4.1;
2. The cap product and the duality map, derived from disks with one positive and two negative corners in Section 4.2; and
3. The inverse to the duality map, given by disks with two positive corners. This is just the η map described in the previous section.

These ingredients will be combined to prove Theorem 1.1 in Section 4.3.

4.1. The Fundamental Class. In Morse theory, the fundamental class is represented by the sum of the maxima of a Morse function. Analogously, the longest Reeb chords — that is, those coming from the right cusps in a resolved plat diagram — should give the fundamental class in the linearized DGA. This is not quite accurate, however, as the change of variables given by an augmentation can introduce new terms. The end result is the following, which will be proved by a direct construction in Section 5.3.

Proposition 4.1. *If the crossings coming from the right cusps of a plat diagram of K are labeled q_{c_1}, \dots, q_{c_r} , then there exists an element $\kappa \in Q^0$, homogeneous of degree 1, of the form*

$$\kappa = q_{c_1} + \dots + q_{c_r} + w,$$

where w does not have any of the q_{c_j} as a summand, that represents a nontrivial homology class in $H_1(A, \partial_1)$.

The class $[\kappa]$ is the **fundamental class** of the knot.

Example. The knot in Figure 2 has a fundamental class consisting purely of the right cusps: $\kappa = q_8 + q_9$. In contrast, it is possible to calculate that the figure 8 knot in Figure 9 has a fundamental class of $\kappa = q_5 + q_7 + q_8 + q_9$ for any augmentation.

Remark 4.2. There is a connection between the fundamental class $[\kappa]$ and the fundamental class of the knot. Using the techniques of Section 5, below, it is possible to prove that the boundaries of the totally augmented disks in $\partial(\kappa)$ pass through each point of $\pi_l(K) \setminus \{\text{double points}\}$ an odd number of times. As a result, $\widehat{\partial}_Q(\tau(\kappa)) = \sum_i c_i^1$, so $\tau(\kappa)$ is no longer a cycle in $(Q^1, \widehat{\partial}_Q)$. In particular, its boundary is the sum of the c generators, i.e., the fundamental class of the circle. In a sense, then, the fundamental class κ in $(Q^0, \widehat{\partial}_Q)$ has been pushed down to degree -1 (in the form of the class defined by the d generators) in $(Q^1, \widehat{\partial}_Q)$.

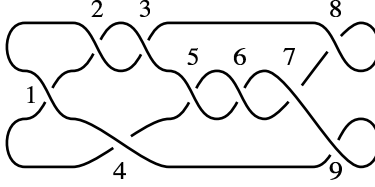


FIGURE 9. The front diagram of a Figure 8 knot whose fundamental class does not consist solely of right cusps in any augmentation.

As Chekanov notes in [4, §12], “closing” a long Legendrian knot induces a one-to-one correspondence between Legendrian isotopy classes of long Legendrian knots and those of Legendrian knots. He also proved that the mapping from the set of Poincaré-Chekanov polynomials for a long Legendrian knot to the set for its closure defined by

$$P(t) \longmapsto P(t) + t$$

is bijective. In particular, there is always a nontrivial homology class in degree 1, i.e., a fundamental class. Chekanov’s construction, however, is not explicit enough for the needs of this paper. The following proposition, which will be important for the proof of duality, relies on the constructions in Section 5:

Proposition 4.3. *If $q \in Q^1$, then*

$$\langle \eta(q), \kappa \rangle = 0.$$

4.2. The Cap Product. As argued in Section 1.2, the cap product for linearized Legendrian contact homology should come from disks with one positive corner and two negative corners. As with the fundamental class, the augmentation interferes with this geometric description, but the length 2 differential, $\widehat{\partial}_2$, encodes the relevant algebraic information.⁴ Geometrically, the length 2 differential counts disks with one positive corner, two negative corners, and possibly other augmented negative corners.

The length 2 differential $\widehat{\partial}_2$ can be split into components just as $\widehat{\partial}_1$ was in Section 3.2. For now, only the components of $\widehat{\partial}_2$ with domain P are of interest; they are:

1. $\Phi_{QP} : P \rightarrow Q \otimes P$,
2. $\Phi_{PQ} : P \rightarrow P \otimes Q$, and
3. $\Phi_{PP} : P \rightarrow P \otimes P$.

That these are the only components follows from the same arguments as in Section 3.2.

Pairing the second tensor factor of Φ_{QP} with the fundamental class turns this map into a “cap product”. More precisely:

⁴Recall that the superscript $\widehat{\varepsilon}$ has been dropped from the notation for the augmented differential.

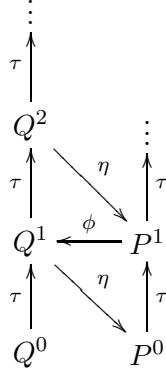


FIGURE 10. Relationships between the maps and spaces defined in Sections 3.2 and 4.2.

Definition 4.4. The **evaluation map** $\text{ev} : P \rightarrow \mathbb{Z}/2$ is defined by

$$\text{ev}(p) = \langle p, \kappa \rangle$$

on P^0 and is extended to all of P by 0.

The **cap product map** $\phi : P \rightarrow Q$ is defined by

$$\phi = (1 \otimes \text{ev})\Phi_{QP}.$$

Note that the terms involved in the power series definition of Φ_{QP} have $\nu = 0$. Thus, the only component of Φ_{QP} involved in the definition of ϕ is $Q^m \otimes P^0$, so ϕ preserves level. The maps and spaces defined thus far can be organized into the diagram in Figure 10.

Lemma 4.5. 1. *The evaluation map descends to $H_*(P, \widehat{\partial}_P)$, i.e., $\text{ev} \circ \widehat{\partial}_P = 0$.*

2. *The cap product map ϕ is a chain map of degree 1.*

Proof. To prove the first part of the lemma, simply compute as follows:

$$\begin{aligned} \text{ev} \circ \widehat{\partial}_P(p) &= \langle \widehat{\partial}_P(p), \kappa \rangle \\ (4.1) \quad &= \langle p, \widehat{\partial}_Q(\kappa) \rangle \text{ by Lemma 3.10} \\ &= 0 \quad \text{by Proposition 4.1.} \end{aligned}$$

The proof of the second part of the lemma comes from looking at the length 2 component of the equation $\widehat{\partial}^2 = 0$:

$$\widehat{\partial}_1 \widehat{\partial}_2 + \widehat{\partial}_2 \widehat{\partial}_1 = 0,$$

and more specifically, the component of the left hand side that maps P to $Q \otimes P$:

$$(4.2) \quad \Phi_{QP} \widehat{\partial}_P + \left(\widehat{\partial}_Q \otimes 1 + 1 \otimes \widehat{\partial}_P \right) \Phi_{QP} = 0.$$

Applying the evaluation map to equation (4.2) yields:

$$(4.3) \quad (1 \otimes \text{ev})\Phi_{QP}\widehat{\partial}_P + \left(\widehat{\partial}_Q \otimes \text{ev} + 1 \otimes (\text{ev} \circ \widehat{\partial}_P)\right)\Phi_{QP} = 0.$$

The first term is simply $\phi\widehat{\partial}_P$, the second term is $\widehat{\partial}_Q\phi$, and the last term vanishes by (4.1). Thus, equation (4.3) reduces to

$$\phi\widehat{\partial}_P + \widehat{\partial}_Q\phi = 0,$$

as desired.

The fact that ϕ is a degree 1 map follows from the facts that Φ_{QP} has degree -1 (it is derived from $\widehat{\partial}$) and ev has degree 2 (it is nonzero only on degree -2 generators in P^0 dual to the degree 1 class κ). \square

Example. A computation similar to that in (3.5) shows that

$$\widehat{\partial}_2 p_7^1 = q_6^1 p_9^0 + p_8^0 q_6^1 + p_7^0 d_3^1 + d_8^1 p_7^0.$$

Only the first term contributes to ϕ :

$$(4.4) \quad \phi_*[p_7^1] = [q_6^1].$$

Note that combining equations (3.13) and (4.4) yields $\tau_*\eta_*\phi_*[p_7^1] = [p_7^1]$.

4.3. Duality. The Morse theoretic motivation, as well as the example above, suggests that $\eta_*\tau_*$ — or, equivalently, $\tau_*\eta_*$ — inverts ϕ_* . This is indeed the case, and it will lead directly to a proof of the main duality theorem.

Proposition 4.6. $\phi_* : H_k(P^1, \widehat{\partial}_P) \rightarrow H_{k+1}(Q^1, \widehat{\partial}_Q)$ is an isomorphism with inverse $\eta_*\tau_* = \tau_*\eta_*$.

Proof. It suffices to find chain homotopies $H : P^1 \rightarrow P^1$ and $K : Q^1 \rightarrow Q^1$ such that

$$(4.5) \quad \tau\eta\phi + Id_{P^1} = H\widehat{\partial}_P + \widehat{\partial}_P H$$

and

$$(4.6) \quad \phi\eta\tau + Id_{Q^1} = K\widehat{\partial}_Q + \widehat{\partial}_Q K.$$

First, define H by:

$$H = \tau(1 \otimes \text{ev})\Phi_{PP}.$$

To prove that H is a chain homotopy between $\tau\eta\phi$ and the identity on P^1 , consider the $P^1 \rightarrow P^0 \otimes P^0$ component of $\widehat{\partial}^2 = 0$:

$$\Phi_{PP}\widehat{\partial}_P + (\widehat{\partial}_P \otimes 1 + 1 \otimes \widehat{\partial}_P)\Phi_{PP} + (\eta \otimes 1)\Phi_{QP} + (1 \otimes \eta)\Phi_{PQ} = 0.$$

Composing with $\tau(1 \otimes \text{ev})$ and using Lemmas 3.9 and 4.5 yields

$$H\widehat{\partial}_P + \widehat{\partial}_P H + \tau\eta\phi + \tau(1 \otimes \text{ev}\eta)\Phi_{PQ} = 0.$$

Thus, it suffices to prove that $\tau(1 \otimes \text{ev}\eta)\Phi_{PQ}$ is the identity on P^1 . Suppose, for a moment, that d^1 lies on a loop corresponding to one of the right

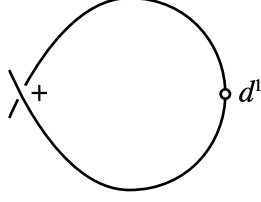


FIGURE 11. The rightmost loop that contains d^1 in the proof of Theorem 4.6.

cusps in a plat diagram, as shown in Figure 11.⁵ Let q^0 and p^0 denote generators coming from the crossing in Figure 11. By Proposition 4.1, q^0 is a summand of κ . Further, $\eta(d^1) = p^0$. Since p^0 pairs nontrivially with q^0 , it follows that $\text{ev } \eta(d^1) = \text{ev}(p^0) = 1$. In general, since all d^1 generators are in the same homology class,

$$(4.7) \quad \text{ev } \eta(\bar{d}^1) = 1$$

for any \bar{d}^1 .

Now let p^1 be any element of P^1 , and consider the second entry in $\tau(1 \otimes \text{ev } \eta)\Phi_{PQ}(p^1)$. Since the first term of Φ_{PQ} must be in P^0 , the second must lie in Q^1 . The external differential contributes terms ending in q^1 or c^1 to $\Phi_{PQ}(p^1)$. In the first case, Lemma 4.3 implies that $\eta(q^1)$ evaluates to 0 on the fundamental class. In the second case, $\eta(c^1)$ has degree -1 , and hence must evaluate to 0 on the fundamental class. In either case, therefore, the external differential makes no nonzero contributions to $\tau(1 \otimes \text{ev } \eta)\Phi_{PQ}(p^1)$. On the other hand, the internal differential always contributes a term of the form $p^0 d^1$ to $\Phi_{PQ}(p^1)$. Combining the internal and external differentials yields:

$$(4.8) \quad \begin{aligned} \tau(1 \otimes \text{ev } \eta)\Phi_{PQ}(p^1) &= \tau(1 \otimes \text{ev } \eta)(p^0 d^1 + \cdots) \\ &= \tau(p^0 \cdot 1) \\ &= p^1, \end{aligned}$$

which proves that $\tau(1 \otimes \text{ev } \eta)\Phi_{PQ}(p^1)$ is the identity on P^1 , and hence that (4.5) holds.

The definition of K and the proof of (4.6) is almost identical to the above, though the relevant component of $\hat{\partial}^2$ is the one from $Q^1 \rightarrow Q^0 \otimes Q^1$. \square

All of the pieces are now in place to prove the duality theorem.

⁵Section 6.1 of [22] guarantees that, without loss of generality, such a d^1 exists.

Proof of Theorem 1.1. First suppose that $|k| > 1$:

$$\begin{aligned}
 \dim H_k(A, \partial) &= \dim H_{-k-1}(P^0, \widehat{\partial}_P) && \text{By Lemma 3.10} \\
 &= \dim H_{-k-1}(P^1, \widehat{\partial}_P) && \text{By Lemma 3.9} \\
 &= \dim H_{-k}(Q^1, \widehat{\partial}_Q) && \text{By Proposition 4.6} \\
 &= \dim H_{-k}(A, \partial) && \text{By (3.10) or (3.12).}
 \end{aligned}$$

The proof of the case where $|k| = 1$ is exactly the same up until the last step, where (3.11) implies that

$$\dim H_1(A, \partial) = \dim H_{-1}(Q^1, \widehat{\partial}_Q) = \dim H_{-1}(A, \partial) + 1,$$

as required by the theorem. Finally, $\dim H_0(A, \partial)$ does not matter for Theorem 1.1, so, modulo the proofs of Propositions 4.1 and 4.3, the proof is complete. \square

5. DIPPED DIAGRAMS AND THE FUNDAMENTAL CLASS

The construction of the fundamental class relies upon Fuchs' philosophy of using Legendrian isotopy to modify the Lagrangian diagram so that the differential becomes simple at the expense of adding many more generators; see [14]. This somewhat technical section realizes Fuchs' philosophy using the techniques of [23], namely by adding "dips" to a resolution of a plat diagram; see Section 5.1. These dips, in turn, allow for the translation of a given augmentation into a special "minimal" augmentation that is closely related to a ruling of the front diagram; see Section 5.2. Finally, in Section 5.3, the fundamental class will be constructed using the minimal augmentation and the ruling, with proofs of Propositions 4.1 and 4.3 following.

5.1. Dipped Plat Diagrams. To put a **dip** in the resolution of a plat diagram, consider the small planar isotopy pictured in Figure 12(a). The valleys in the front diagram are nested and increasingly sharp from bottom to top. This means that the changes in the y -coordinates are increasingly drastic; in particular, the bottom strand does not move in the Lagrangian diagram, while the y -coordinate of the top strand dives down sharply and then returns quickly back. Since the z -coordinates have not changed much, the top strand still lies above all other strands in the Lagrangian diagram. The result for the Lagrangian diagram is pictured in Figure 12(b).

Each dip introduces a slew of new generators. Suppose that the dip occurs between the crossings q_j and q_{j+1} . Number the strands from bottom to top. The crossing between strand k and strand l ($k > l$) in the left-hand half-lattice is denoted b_{kl}^j , whereas the corresponding crossing in the right-hand half-lattice is denoted a_{kl}^j . Note that if the dip occurs between the left cusps and q_1 , then the new crossings are labeled with a superscript 0; if the dip occurs between the last crossing q_n and the right cusps, then the new crossings are labeled with a superscript n . Placing dips in strategic locations will facilitate the construction of the fundamental class.

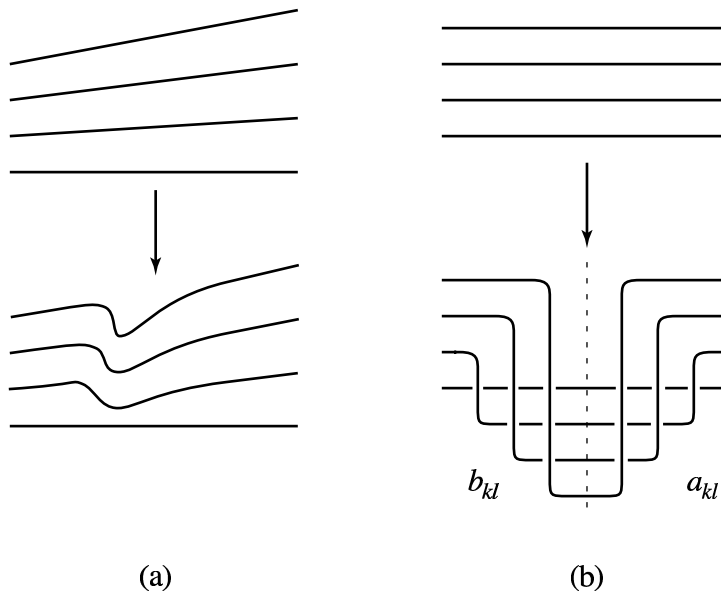


FIGURE 12. (a) The small planar isotopy in a resolved front diagram that leads to the “dips” in the Lagrangian diagram shown in (b).

Definition 5.1. A **dipped diagram** of a Legendrian knot is the Lagrangian diagram that results from taking a plat diagram and placing a dip just to the right of the left cusps, just to the left of the right cusps, and between any two consecutive crossings.

After a full set of dips is in place, it is straightforward to write out the differentials of the a^j and b^j generators for $1 < j < n$. The key feature is that all disks are “local,” i.e., no disk can pass through a dip. The immersion property in Definition 2.1 implies that there can be four possible types of disks, shown in Figure 13:

1. “Long” disks that run between the b^j and a^{j-1} lattices.
2. “Short” disks that run between the b^j and a^j lattices,
3. Disks that lie entirely inside the a^{j-1} -lattice, and
4. Disks that lie entirely inside the b^j -lattice.

The combinatorics of the dipped diagram place further restrictions on the pattern of positive and negative corners for each of these disks. Disks of type (1) and (2) that contribute to the differential must have a positive corner (and possibly a negative corner) in the b^j lattice and exactly one negative corner in the a^{j-1} or a^j lattices, respectively. Disks of type (3) must have exactly two negative corners, and disks of type (4) cannot contribute to the differential, though they will make an appearance in Section 5.4.

5.2. Rulings and Minimal Augmentations. The construction of a minimal augmentation on a dipped diagram requires a side trip into the realm of

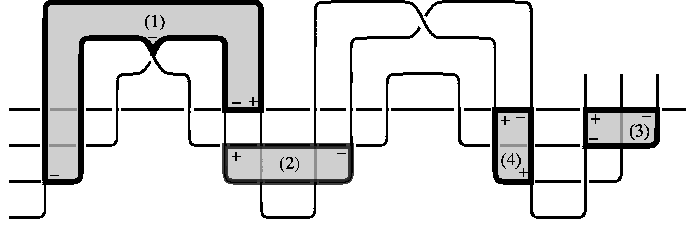


FIGURE 13. The four types of disks in a dipped diagram that the immersion property allows.

rulings of front diagrams; see [5, 6, 14]. Suppose that a Legendrian knot K has a front diagram whose singular values all have distinct x coordinates. A **ruling** consists of a one-to-one correspondence between the set of left cusps and the set of right cusps and, for each pair of corresponding cusps, two paths in the front diagram that join them. The ruling paths must satisfy the following conditions:

1. Any two paths in the ruling meet only at crossings or at cusps; and
2. The interiors of the two paths joining corresponding cusps are disjoint, and hence they meet only at the cusps and bound a topological disk.

Note that these disks are similar to those used to define the differential ∂ , but they may have “obtuse” corners; see Figure 14(S2), for example.

As Fuchs notes, these conditions imply that the paths cover the front diagram and the x coordinate of each path in the ruling is monotonic.

At a crossing, either the two ruling paths incident to the crossing pass through each other or one path lies entirely above the other. In the latter case, say that the ruling is **switched** at the crossing. Near a crossing, call the two ruling paths that intersect the crossing **crossing paths** and the ruling paths that are paired with the crossing paths **companion paths**. If all of the switched crossings of a ruling are of types (S1–3) in Figure 14, then the ruling is **normal**. If all of the switched crossings have grading 0, then the ruling is **graded**.

That there is a connection between rulings and augmentations was first discovered by Fuchs [14], who proved that the existence of a normal ruling implies the existence of an augmentation. The converse was proved in [15, 23]:

Theorem 5.2 ([14, 15, 23]). *For a given Legendrian knot K , a graded augmentation of the contact homology DGA exists if and only if every front diagram of K has a graded normal ruling.*

As described in [20], the construction of the ruling from an augmentation can be rendered algorithmic. The algorithm also yields a **virtual augmentation** ε_{vir} on the plat diagram. This virtual augmentation is nonzero on the switched crossings (S1–3) of Figure 14, zero on the “departures” (D1–3), and possibly nonzero on the “returns” (R1–3).

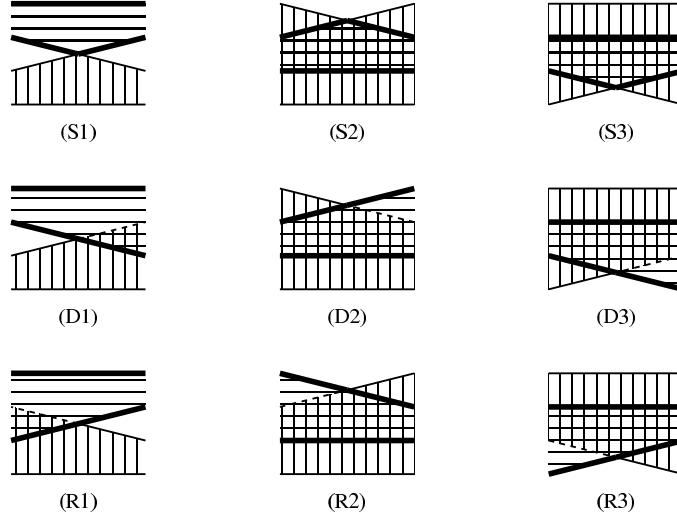


FIGURE 14. The possible configurations of a normal ruling near a crossing. Only the crossing paths and their companions are shown.

Definition 5.3. Given an augmentation and its corresponding graded normal ruling and virtual augmentation on a plat diagram, the corresponding **minimal augmentation** ε_m for the dipped diagram satisfies the following properties in the dip between q_j and q_{j+1} :

1. a_{kl}^j is augmented if and only if the strands k and l are paired in the portion of the ruling that lies between q_j and q_{j+1} , where q_0 and q_{n+1} are understood to be the left and right cusps, respectively.
2. For the leftmost dip, no b_{kl}^0 is augmented.
3. Let $\varepsilon_m(q_j) = \varepsilon_{\text{vir}}(q_j)$. Let b_x^j be the b_{kl}^j generator corresponding to the crossing strands of q_j and let b_c^j correspond to the companion strands. The augmentations of these generators depend on the configuration of the ruling at q_j . If $\varepsilon_m(q_j) = 0$ — for example, if q_j is a departure — then neither b_x^j nor b_c^j is augmented. Otherwise:

Configuration	Augmented Crossings
S1	b_x^j
S2, S3	b_x^j and b_c^j
R1	None
R2, R3	b_c^j

No other b_{kl}^j is augmented.

Since the dipped and plat diagrams come from Legendrian isotopic knots, the DGAs $(\mathcal{A}_{\text{dip}}, \partial_{\text{dip}})$ and (\mathcal{A}, ∂) must be stable tame isomorphic. Let $S(\mathcal{A})$ be the result of many stabilizations of \mathcal{A} , and let $\psi : \mathcal{A}_{\text{dip}} \rightarrow S(\mathcal{A})$ be the DGA isomorphism constructed in the proof of Theorem 5.2 in [23]. Then a

lift $\tilde{\varepsilon}$ of ε to $S(\mathcal{A})$ and ε_m correspond under ψ as in (2.2). The argument in Section 2.3 then implies that if ε is an augmentation for a plat diagram of K and ε_m is the corresponding minimal augmentation for the dipped diagram, then $\psi^\varepsilon = \Phi^{\tilde{\varepsilon}}\psi(\Phi^{\varepsilon_m})^{-1}$ restricts to a *linear* chain isomorphism.

5.3. The Fundamental Class of a Dipped Diagram. All of the background is now in place to prove Proposition 4.1. The strategy is to construct a fundamental class κ_{dip} on the dipped diagram and then to transfer the result back to the original knot.

Definition 5.4. The **dipped fundamental class** $[\kappa_{\text{dip}}]$ is represented by the sum of the following crossings in a ruled dipped diagram:

1. All crossings coming from right cusps;
2. In the j^{th} dip, all crossings b_{kl}^j such that the strands k and l are paired in the portion of the ruling that passes through the dip; and
3. Crossings that depend on the configuration of the ruling at q_j if $\varepsilon_m(q_j) = 1$. These contributions are as follows: suppose that the crossing strands are labeled i and $i + 1$ and that the companion strands are labeled K and L with $K < L$.

Configuration	Additional Generators
S1, R1	a_{LK}^{j-1}
S2	b_{iK}^j
S3, R3	b_{Ki}^j
R2	None

The **fundamental class** $[\kappa]$ is the image of $[\kappa_{\text{dip}}]$ under the map induced by the linearization of $\pi\psi^\varepsilon$.

As in the statement of Proposition 4.1, let q_{c_1}, \dots, q_{c_r} be the crossings coming from right cusps. By the first condition of the definition above, κ_{dip} is of the form

$$\kappa_{\text{dip}} = \sum_j q_{c_j} + w,$$

where w is a sum of non-right-cusp crossings. The isomorphism $\psi : \mathcal{A}_{\text{dip}} \rightarrow S(\mathcal{A})$ mentioned in the previous section comes from a composition of maps induced by Type II Reidemeister moves; see Section 3.2 of [23]. These maps modify the generators coming from right cusps by adding on words in generators of strictly smaller height — that is, in generators lying strictly to the left of the right cusps in the plat diagram. When linearized, these constituent maps will take each generator coming from a right cusp in the dipped diagram to the sum of such a generator in the plat diagram with crossings lying strictly to its left. As a consequence, the image of κ_{dip} still contains the sum of the right cusps. Proposition 4.1 is thus reduced to the following lemma:

Lemma 5.5. *The element κ_{dip} (and hence κ) represents a nontrivial linear homology class of grading 1.*

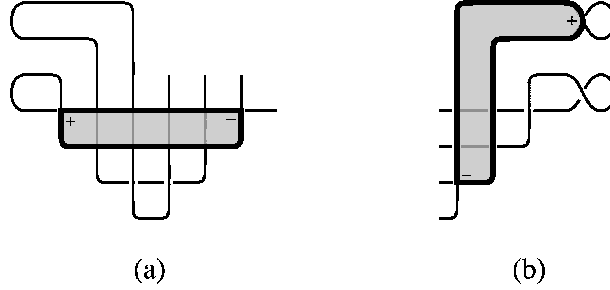


FIGURE 15. (a) The type of disk that gives the linearized differential of a generator near a left cusp; (b) the type of disk that gives the linearized differential of a generator coming from a right cusp.

Proof. In what follows, let $\tilde{\partial}$ denote the linearized differential on the dipped diagram that comes from the minimal augmentation.

The first claim implicit in the proposition is that κ_{dip} is a linear cycle of degree 1. To prove it, begin by examining the left and right ends of a plat diagram. At both ends, the strands $2i - 1$ and $2i$ are paired in the ruling. On the right, the linearized differential of the crossing that corresponds to a right cusp that joins these strands is simply $a_{2i,2i-1}^n$. On the left, the linearized differential of the crossing $b_{2i,2i-1}^1$ is $a_{2i,2i-1}^1$. See Figure 15. In all, the crossings a_*^1 and a_*^n between strands paired in the ruling — to be referred to as “paired crossings” henceforth — generate the image of the linearized differential of the summands of κ_{dip} that lie at the extreme right and left of the dipped diagram.

In general, denote by κ^j the summands of κ_{dip} that lie in the j^{th} dip, including the a_{LK}^{j-1} generators in configurations (S1) and (R1). In light of the analysis above, it suffices to show that, for $1 < j \leq n$, $\tilde{\partial}\kappa^j$ is the sum of all paired crossings a_*^j and a_*^{j-1} . The remainder of the proof is, essentially, a case-by-case verification of this fact, using the four types of disks discussed at the end of Section 5.1 and shown in Figure 13.

In all configurations except (S2) and (S3), the ruling disks induce totally augmented⁶ type (1) and type (2) disks that contribute to the differential of the paired b_*^j crossings in κ^j . For the departure and return configurations, and for the ruling disks not involved in the crossing in the switched configurations, these disks have exactly one negative corner at a paired crossing in the a^{j-1} lattice. In configuration (S1), both switched disks have an additional corner at q_j , and hence these terms cancel in $\tilde{\partial}\kappa^j$, leaving only the paired crossings in the a^{j-1} lattice. In configuration (S2), the ruling disks induce totally augmented type (1) and type (2) disks in $\tilde{\partial}\kappa^j$ as before, with the exception of the “outer disk” that has a concave corner. It would appear,

⁶Recall that a disk is “totally augmented” if all of its negative corners are augmented.

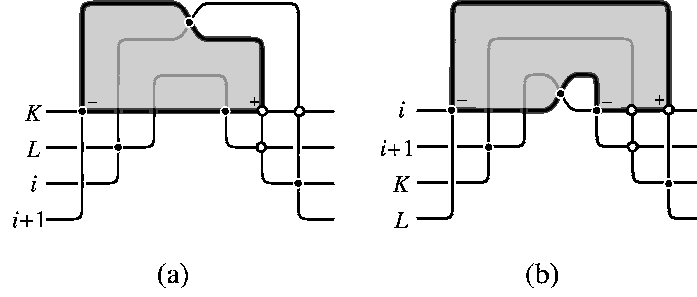


FIGURE 16. The “extra” disks in configurations (a) (S2) and (b) (S3) that replaces the disk induced from the ruling. Open dots indicate summands of κ_{dip} and closed dots indicate augmented corners.

then, that a_{Li}^{j-1} is not in the image of $\tilde{\partial}\kappa^j$ and that $\tilde{\partial}\kappa^j$ has an extra q_j term. However, there is a disk with its positive corner at b_{iK}^j that has a negative corner at $a_{i+1,K}^{j-1}$; see Figure 16(a). The extra q_j term that comes from the inner ruling disk involved in the switch will be canceled by disks considered below. The extra disk in configuration (S3) comes from the differential of b_{Li}^j as it would if it were the outer disk, but it has an extra (augmented) negative corner at $b_{i+1,i}^j$; see Figure 16(b). Again, this extra corner and the extra q_j from the inner disk will be canceled by disks considered below.

Note that the fact that the differential of crossings b_*^j between strands paired in the ruling contains a totally augmented disk implies that the degree of the b_*^j crossings in κ^j is 1.

If $\varepsilon_m(q_j) = 0$ — in particular, in departure and some return configurations — then there are no other disks that contribute to the linearized differential, and the proof is complete. If $\varepsilon_m(q_j) = 1$, then there are more disks to consider. The terms that these disks contribute, however, cancel out, just leaving the paired a^{j-1} and a^j crossings found above. In configuration (S1), there are type (1) disks that contribute the additional terms a_{Li}^{j-1} and $a_{i+1,K}^{j-1}$. In configuration (R1), the additional terms are $a_{L,i+1}^{j-1}$ and a_{iK}^{j-1} . In both of these configurations, the extra terms are canceled precisely by type (3) disks whose positive corner lies at a_{LK}^{j-1} . See Figure 17(a) for the (S1) case. Incidentally, since $|b_*^j| = 1$, this proves that $|a_{LK}^{j-1}| = 1$ in these configurations as well.

In configuration (R2), the differentials of the b_*^j include terms that come from two extra disks, but they both contribute a_{iL}^{j-1} ; see Figure 17(b). Configuration (R3) also has two additional disks between the $(j-1)^{\text{st}}$ and j^{th} dips, one with positive corner at $b_{K,i+1}^j$ and another with positive corner at b_{Ki}^j , whose contributions cancel. In addition, in configuration (R3), there

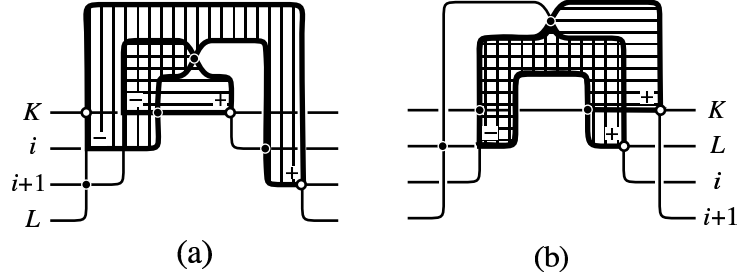


FIGURE 17. Extra type (1) disks that contribute terms to $\tilde{\partial}\kappa^j$ in configurations (a) S1 and (b) R2.

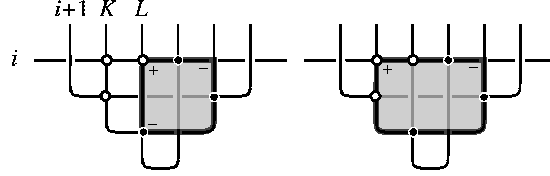


FIGURE 18. Extra type (2) disks that contribute terms to $\tilde{\partial}\kappa^j$ in configurations (S2), (S3), and (R3). The strand labels come from the (R3) case.

are two extra disks inside the j^{th} dip, though, again, their contributions cancel, as shown in Figure 18.

There are also extra disks in configurations (S2) and (S3). For (S2), $\tilde{\partial}b_{Ki}^j$ contributes a totally augmented disk with negative corners at q_j (which cancels the leftover q_j from above), a_{iL}^{j-1} , and b_{LK}^j (both canceled by a totally augmented disk with positive corner at $b_{i+1,K}^j$). There are two disks that are not totally augmented that both contribute $a_{i+1,L}^{j-1}$, one with positive corner at b_{iL}^j and the other with positive corner at b_{iK}^j . As in configuration (R3), there are additional disks inside the j^{th} dip, and they cancel in the same way. The argument that terms from the extra disks cancel out (and cancel the additional $b_{i+1,i}^j$ from the replacement for the ruling disk) for configuration (S3) is similar to that for configuration (S2). This completes the proof that κ_{dip} is a linear cycle of degree 1.

The proof that κ_{dip} is not a boundary is quite a bit easier: it is clear that no disk can have a negative corner at any of the crossings that correspond to the right cusps, so these terms can never appear in the image of the linearized differential. \square

5.4. Proof of Proposition 4.3. Proposition 4.3 can be reformulated in terms of disks in a dipped diagram with a minimal augmentation as follows:

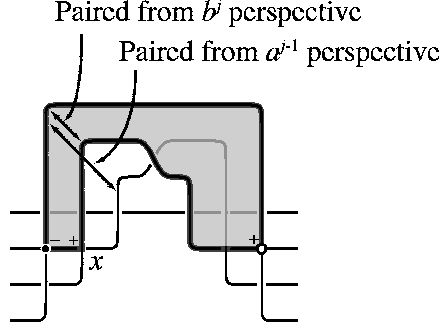


FIGURE 19. The form of a potential disk of type (1) in $\Delta^+(x)$ in the case that $\varepsilon_m(q_j) = 0$.

Lemma 5.6. *Let x be a crossing of the dipped diagram, and let $\Delta^+(x)$ be the set of immersed disks up to reparametrization that satisfy the criteria of Definition 2.1 except for the following conditions at the corners:*

1. *The disk has exactly two positive corners, one of which is at x and the other of which is at a summand of κ_{dip} ; and*
2. *All other corners of the disk are negative and augmented.*

The number of disks in $\Delta^+(x)$ is even.

Proof. Like the proof of Lemma 5.5, this proof comes down to checking the lemma for each configuration in Figure 14 using the four types of disks in Figure 13. As in the discussion at the end of Section 5.1, the combinatorics of the dipped diagram place restrictions on the pattern of positive and negative corners for each of these disks. Disks of types (1) and (2) can have at most one positive corner in each lattice. Further, disks of types (3) and (4) must have at least three corners, and hence must have at least one negative augmented corner in order to appear in $\Delta^+(x)$ for some x . In fact, in a type (3) disk, there must be four corners in order for there to be two positive ones.

The proof proceeds by cases. First suppose that $\varepsilon_m(q_j) = 0$. In this case, the sets $\Delta^+(x)$ will be empty for all x . Consider a disk of type (1). Since there are no summands of κ_{dip} in the a^{j-1} lattice, x must lie in the a^{j-1} lattice, along with an augmented negative corner; see Figure 19. At the negative corner, the horizontal and vertical strands must be paired in the ruling. Thus, the two vertical strands on the boundary of the disk in the a^{j-1} lattice are *not* paired. This implies that the strands on the boundary of the disk as it enters the b^j lattice are not paired. In the b^j lattice, however, there are no augmented crossings, so the disk must have only one (positive) corner there, as shown in Figure 19. This corner is a summand of κ_{dip} , so it must be at a paired crossing. This is a contradiction, so the set $\Delta^+(x)$ is empty in this case.

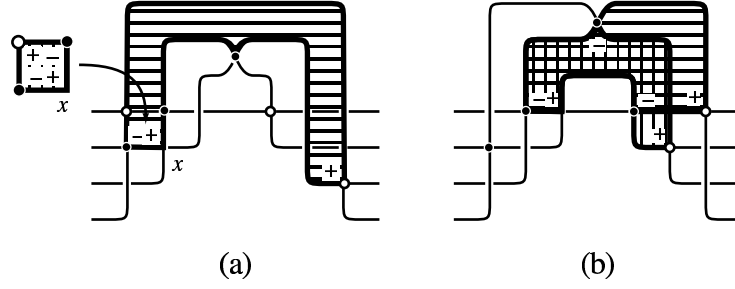


FIGURE 20. Type (1) disks and the disks that cancel them in configurations (a) (R1) and (b) (R2).

Next, consider a disk of type (2). This disk must have a positive corner in each lattice and a negative corner in the a^j lattice that lies above the positive corner. As before, x must lie in the a^j lattice: the only way for a summand of κ_{dip} to lie in the a^j lattice is if the configuration to the right of the a^j lattice is (S1) or (R1). Denote the positive corner in the b^j lattice by b_{kl} , where the strands k and l are paired in the ruling. The negative corner in the a^j lattice is of the form a_{ml} for some $m > l$. Since it must be augmented, and only crossings between paired strands in the a^j lattice are augmented, it follows that $m = k$. Thus, the positive corner in the a^j lattice is of the form a_{kn} for some $n < k$. It follows that the disk must have a negative corner at b_{kn} . Since there are no augmented corners in the b^j lattice, this disk does not satisfy the second condition for $\Delta^+(x)$.

Finally, consider disks of type (3) or (4). Since $\varepsilon_m(q_j) = 0$, Definition 5.4 implies that there are no summands of κ_{dip} in the a^{j-1} lattice, so no disks of type (3) can appear. Since there are no augmented corners in the b^j -lattice, no disks of type (4) can appear. This completes the argument in the case that $\varepsilon_m(q_j) = 0$.

Next, suppose that $\varepsilon_m(q_j) = 1$, and consider disks of type (1). As when $\varepsilon_m(q_j) = 0$, the crossing x must lie in the a^{j-1} lattice and the summand of κ_{dip} must lie in the b^j lattice; this even holds in configurations (S1) and (R1) since there are no augmented crossings to the left of a_{LK}^{j-1} . If neither or one of the strands on the boundary between the a^{j-1} and b^j lattices is a crossing or a companion strand, then the same argument as for the $\varepsilon_m(q_j) = 0$ case applies. Thus, only disks involving the crossing and companion strands need be considered. It can be checked directly that there are no disks in $\Delta^+(x)$ in configuration (S1). In configuration (R1), there is one type (1) disk that is canceled by a type (3) disk; see Figure 20(a). In all other configurations with $\varepsilon_m(q_j) = 1$, the type (1) disks come in pairs; see Figure 20(b) for the case of (R2).

For a disk of type (2) to lie in $\Delta^+(x)$, one of two conditions must hold: either the summand of κ_{dip} is not a crossing between paired strands, or there is an augmented corner directly below a summand of κ_{dip} in the b^j

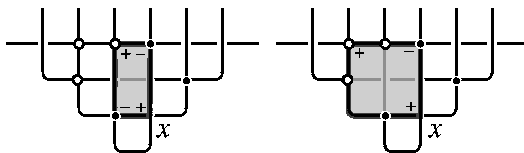


FIGURE 21. Canceling type (2) disks in configurations (S2), (S3), and (R3).

lattice. Otherwise, the $\varepsilon_m(q_j) = 1$ situation is exactly the same as that of $\varepsilon_m(q_j) = 0$. The conditions are satisfied only in configurations (S2), (S3), and (R3), and in these configurations, *both* conditions are satisfied. As shown in Figure 21, however, precisely two disks of type (2) exist in these configurations, and hence the lemma holds.

Aside from the case of configuration (R1) mentioned above, no disks of type (3) lie in $\Delta^+(x)$. To see this, notice that in configurations (S2), (S3), (R2), and (R3), there are no summands of κ_{dip} in the a^{j-1} lattice. The fact that there are no disks in configuration (S1) can be easily checked directly.

The last step in the proof is to notice that no disk of type (4) lies in Δ^+ . Every disk of type (4) must have an augmented negative corner to the right of the top left positive corner in the b^j lattice; this is never the case. \square

REFERENCES

- [1] D. Bennequin, *Entrelacements et equations de Pfaff*, Asterisque **107–108** (1983), 87–161.
- [2] M. Betz and R. L. Cohen, *Graph moduli spaces and cohomology operations*, Turkish J. Math. **18** (1994), no. 1, 23–41.
- [3] F. Bourgeois, *A Morse-Bott approach to contact homology*, Symplectic and contact topology: interactions and perspectives (Toronto, ON/Montreal, QC, 2001), Fields Inst. Commun., vol. 35, Amer. Math. Soc., Providence, RI, 2003, pp. 55–77.
- [4] Yu. Chekanov, *Differential algebra of Legendrian links*, Invent. Math. **150** (2002), 441–483.
- [5] ———, *Invariants of Legendrian knots*, Proceedings of the International Congress of Mathematicians, Vol. II (Beijing, 2002) (Beijing), Higher Ed. Press, 2002, pp. 385–394.
- [6] Yu. Chekanov and P. Pushkar, *Combinatorics of Legendrian links and the Arnol’d 4-conjectures*, Russ. Math. Surv. **60** (2005), no. 1, 95–149.
- [7] F. Ding and H. Geiges, *Legendrian knots and links classified by classical invariants*, Preprint available on arXiv as math.SG/0503033, 2005.
- [8] Y. Eliashberg, *Invariants in contact topology*, Proceedings of the International Congress of Mathematicians, Vol. II (Berlin, 1998), no. Extra Vol. II, 1998, pp. 327–338 (electronic).
- [9] Y. Eliashberg and M. Fraser, *Classification of topologically trivial Legendrian knots*, Geometry, topology, and dynamics (Montreal, PQ, 1995), Amer. Math. Soc., Providence, RI, 1998, pp. 17–51.
- [10] Y. Eliashberg, A. Givental, and H. Hofer, *Introduction to symplectic field theory*, Geom. Funct. Anal. (2000), no. Special Volume, Part II, 560–673.
- [11] J. Etnyre, *Legendrian and transversal knots*, To appear in the Handbook of Knot Theory, 2003.

- [12] J. Etnyre and K. Honda, *Knots and contact geometry I: Torus knots and the figure eight knot*, J. Symplectic Geom. **1** (2001), no. 1, 63–120.
- [13] J. Etnyre, L. Ng, and J. Sabloff, *Invariants of Legendrian knots and coherent orientations*, J. Symplectic Geom. **1** (2002), no. 2, 321–367.
- [14] D. Fuchs, *Chekanov-Eliashberg invariant of Legendrian knots: existence of augmentations*, J. Geom. Phys. **47** (2003), no. 1, 43–65.
- [15] D. Fuchs and T. Ishkhanov, *Invariants of Legendrian knots and decompositions of front diagrams*, Mosc. Math. J. **4** (2004), no. 3, 707–717.
- [16] K. Fukaya and Y.-G. Oh, *Zero-loop open strings in the cotangent bundle and Morse homotopy*, Asian J. Math. **1** (1997), no. 1, 96–180.
- [17] T. Kálmán, *Contact homology and one parameter families of Legendrian knots*, Preprint available on arXiv as math.GT/0407347.
- [18] P. Melvin and S. Shrestha, *The nonuniqueness of Chekanov polynomials of Legendrian knots*, Geom. Topol. **9** (2005), 1221–1252.
- [19] L. Ng, *Computable Legendrian invariants*, Topology **42** (2003), no. 1, 55–82.
- [20] L. Ng and J. Sabloff, *The correspondence between augmentations and rulings for Legendrian knots*, Pacific J. Math. (2005), To appear.
- [21] J. Sabloff, *Invariants for Legendrian knots from contact homology*, In preparation.
- [22] ———, *Invariants of Legendrian knots in circle bundles*, Comm. Contemp. Math. **5** (2003), no. 4, 569–627.
- [23] ———, *Augmentations and rulings of Legendrian knots*, Int. Math. Res. Not. (2005), no. 19, 1157–1180.
- [24] M. Schwarz, *Morse homology*, Birkhäuser Verlag, Basel, 1993.

HAVERFORD COLLEGE, HAVERFORD, PA 19041

E-mail address: jsabloff@haverford.edu